

Preparation of Superabsorbent Resin from Carboxymethyl Cellulose Grafted with Acrylic Acid by Low-temperature Plasma Treatment

Li Jie Huang,* Ying Yang, Yuan Yuan Cai, Ming Liu, Ting Xu, Guang Zai Nong, and Shuang Fei Wang

A superabsorbent resin (SAR) synthesized from carboxymethyl cellulose (CMC) by grafting acrylic acid (AA) was studied using single-factor analysis. The optimum preparation conditions were as follows: plasma discharge power of 250 W, processing time of 90 s, pressure of 300 Pa, $m(\text{CMC}):m(\text{AA})$ ratio of 1:9, $m(\text{K}_2\text{S}_2\text{O}_8):m(\text{CMC})$ ratio of 1:4, and neutralization degree of 40%. Under these conditions, the resin has a salt water absorbency of 38.5 g/g and a stable chlorine dioxide solution absorbency of 27.2 g/g. The structural characterization of the SAR was also studied by Fourier transform infrared spectroscopy (FTIR), X-ray diffraction (XRD), scanning electron microscopy (SEM), and differential scanning calorimetry (DSC). The results showed that the resin was synthesized by grafting copolymerization of CMC and AA, and the water absorbency and thermal stability of the resin were greatly improved compared to CMC alone. This method may provide a new way for high value-added utilization of bagasse.

Keywords: Low-temperature plasma; Carboxymethyl cellulose; Acrylic acid; Superabsorbent resin

Contact information: College of Light Industry and Food Engineering, Guangxi University, Nanning 530004, Guangxi, China; *Corresponding author: jiely165@163.com

INTRODUCTION

Superabsorbent resin (SAR), as a functional polymer material, has super water absorbency and retention, which can be widely used in agriculture (Liu *et al.* 2013; 2013), health care (Sadeghi and Hosseinzadeh 2008; Maithili and Ram 2003), construction (Song *et al.* 2009), and other industries. SAR can be synthesized from carboxymethyl cellulose with low-temperature plasma treatment, which makes use of a variety of high-energy particles in the plasma to bombard the material surface to realize the graft polymerization of the active groups of CMC and monomers.

The surface modification method has many advantages over the traditional method (Kabiri *et al.* 2003; Miao *et al.* 2012): (1) Cellulose with a low-temperature plasma treatment will no longer require a crosslinking agent, which can reduce environmental pollution. (2) The grafting reaction time is shortened, as there is no need for the reaction to proceed under the protection of nitrogen. (3) It is a green environmental processing technology with a simple process to control the reaction conditions and the operation. This study investigated the effects of different process parameters on the water absorbency of SAR to ensure the optimum conditions and characterize the structure of the product using modern analytical techniques.

EXPERIMENTAL

Materials

Carboxymethyl cellulose (CMC) was obtained from bleached bagasse pulp; the acrylic acid (AA), sodium hydroxide, potassium persulfate, and methanol used in this study were all of analytical grade. Nitrogen with a purity of 99.2% was also used. The CMC was treated by an HPD atmospheric glow discharge plasma system (Nanjing Suman Electronics Co., Ltd.). The functional groups of carboxymethyl cellulose before and after grafting reaction were analyzed by Perkin Elmer BX 95038 FTIR (USA). The crystallinity of bagasse pulp during the etherification and grafting reactions was analyzed using a Ricoh D/MAX-2500 XRD and Hitachi S-3400N SEM (Japan). The thermal stability of carboxymethyl cellulose before and after the grafting reaction was analyzed by an STA409PC integrated thermal analyzer (Netzsch Company, Germany).

Low-temperature Plasma Treatment

The prepared carboxymethyl cellulose was put on a clean watch glass after drying and was then moved to the low-temperature plasma processing chamber. The vacuum degree was set and the vacuum valve was opened. The power and processing time were adjusted after evacuating the vacuum. Finally, the discharge switch was opened and the samples began to graft after the discharge.

Grafting Reaction

After treatment by low-temperature plasma, 2 g of carboxymethyl cellulose was put in 50 mL of deionized water in a three-neck flask. Nitrogen gas was then aerated and certain amounts of NaOH, AA, and $K_2S_2O_8$ (initiator) were added while stirring at 60 °C. After a period of time, a pink viscous liquid was produced, and the product was then dried in vacuum at 60 °C until a constant weight was achieved; the final result was a brown-yellow product.

Water Absorbency Measurement

A set amount of dry sample was accurately weighed (m_1 , g) and immersed in plenty of salt water (9 g/L) and stable chlorine dioxide solution (30.9850 g/L), respectively. After 24 h, the sample was percolated through the liquid using a 100-mesh gauze and then put on filter paper for 5 min to absorb the surface water of the sample. Then, the sample was weighed again (m_2 , g). The water absorbency (Q , g/g) was determined from the following equation (Ma *et al.* 2011),

$$Q = \frac{m_2 - m_1}{m_1} \quad (1)$$

where Q (g/g) is water absorbency, m_1 (g) is the weight of the dry sample, and m_2 (g) is the weight of the sample after absorbing and filtering.

RESULTS AND DISCUSSION

The largest absorbency of the resin was 508.7g/g for deionized water. Because of its high absorbency, the resin is regarded as a superabsorbent resin.

Effect of Low-temperature Plasma Treatment on Water Absorbency

The grafting reaction stage was operated at fixed conditions as follows: $m(\text{CMC}):m(\text{AA})$ ratio = 1:9, $m(\text{K}_2\text{S}_2\text{O}_8):m(\text{CMC})$ ratio = 1:4, and a neutralization degree of 40%. The effect of plasma on the water absorbency was investigated with different discharge powers, treatment times, and pressures.

Effect of plasma discharge power

The effect of different discharge powers on the water absorbency was investigated at a pressure of 500 Pa and treatment time of 90 s.

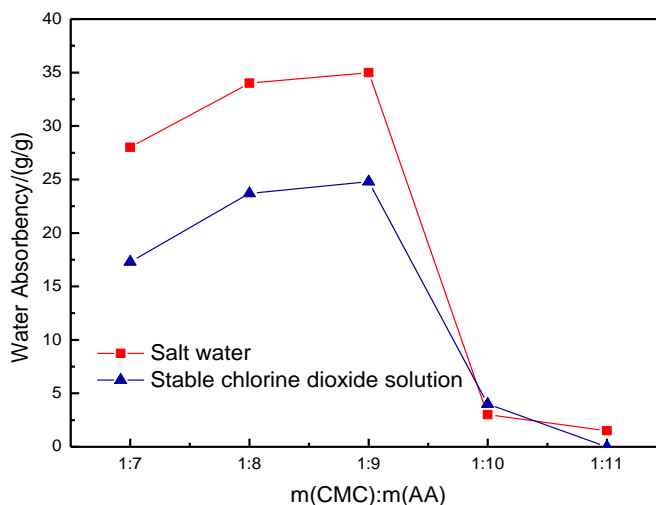


Fig. 1. Effect of discharge power on water absorbency

As shown in Fig. 1, the water absorbency increased with increasing plasma discharge power, up to 250 W. The water absorbency was 36.0 g/g for salt water and 24.5 g/g for stable chlorine dioxide solution and decreased as the power increased above 250 W. This is because the gas content in the plasma chamber was relatively stable at a set pressure, and the increasing discharge power increased the energy available to excite the particles, so the number of free radicals impacted by high-energy active particles also increased. However, when the discharge power was sufficiently high, collisions between high-energy particles also increased, which could decrease the energy and number of active particles. Also, this could intensify the collisions between high-energy particles and the fiber, causing excessive oxidation, crosslinking, and etching of the fiber surface and severe damage to the surface of amorphous regions. Therefore, moderate discharge power was very important for good results. The optimal discharge power was therefore chosen to be 250 W.

Effect of plasma treatment time

The effect of different treatment times on the water absorbency was investigated at a plasma discharge power of 250 W and pressure of 500 Pa.

As shown in Fig. 2, the water absorbency increased with increasing plasma treatment time, up to 90 s. The water absorbency was up to 36.0 g/g for salt water and 24.5 g/g for stable chlorine dioxide solution and decreased as treatment time continued beyond 90 s. This can be attributed to the increasing number of free radicals under a set power. When the free radical density reached a maximum value, the free radical density did not increase significantly, but that does not necessarily mean that there was no new generation of free radicals. Free radicals were in a dynamic equilibrium state (Park *et al.* 2005). With increasing treatment time, the degree of cross-linked reactions on the cellulose surface increased. The optimal treatment time was therefore determined to be 90 s.

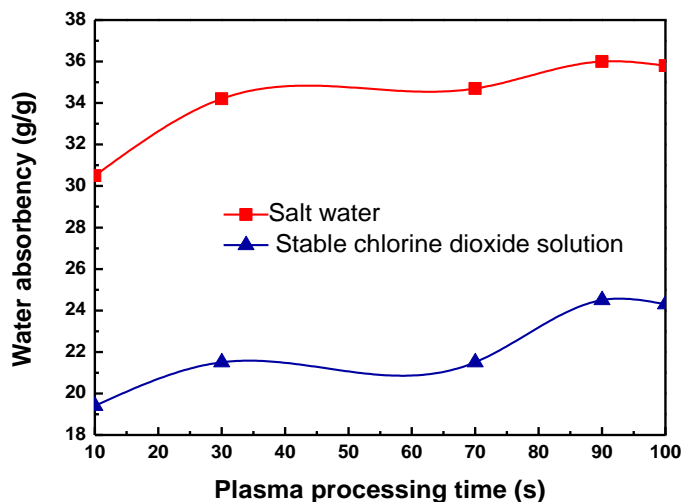


Fig. 2. Effect of plasma processing time on water absorbency

Effect of plasma vacuum degree

The effect of different pressures on the water absorbency was investigated at a plasma discharge power of 250 W and treatment time of 90 s.

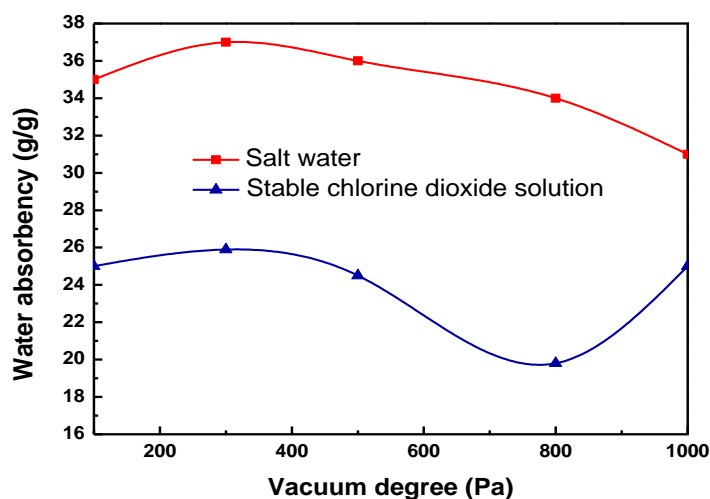


Fig. 3. Effect of vacuum degree on water absorbency

The water absorbency increased with increasing pressure, up to 300 W. The water absorbency was up to 37.0 g/g for salt water and 25.9 g/g for stable chlorine dioxide solution, and it decreased as the pressure continued to increase. This can be explained

because when the pressure was at a low level, the gas density was small and the relative freedom degree of electrons was large, making the collision probability small, and the number of ions, which could be used for excitation as well as free radicals, was reduced. However, if the vacuum degree was too large and the gas density was too high, it caused the collision of particles to increase, resulting in a waste of energy that was not conducive to the grafting reaction. The optimal vacuum degree was therefore chosen to be 300 Pa.

Effect of Grafting Conditions on Water Absorbency

After plasma treatment, the effect of the amount of initiator and AA, and the degree of neutralization in the grafting reaction stage on the water absorbency was investigated. For these experiments, the plasma discharge power was 250 W, the processing time was 90 s, and the pressure was 300 Pa.

Effect of acrylic acid dosage

The effect of the amount of AA on the water absorbency was investigated at a $m(\text{K}_2\text{S}_2\text{O}_8):m(\text{CMC})$ ratio of 1:4 and a degree of neutralization of 40%. The AA dosages were 14, 16, 18, 20, and 22 g; with 2 g of carboxymethyl cellulose. The $m(\text{CMC}):m(\text{AA})$ ratios were therefore 1:7, 1:8, 1:9, 1:10, and 1:11, respectively.

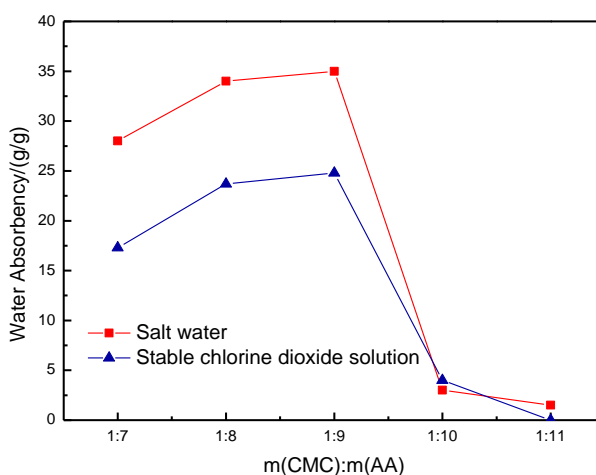


Fig. 4. Effect of $m(\text{CMC}):m(\text{AA})$ on water absorbency

The water absorbency increased with increasing AA dosage. When the $m(\text{CMC}):m(\text{AA})$ ratio was 1:9, the water absorbency was up to 35.0 g/g for salt water and 24.8 g/g for stable chlorine dioxide solution, but with further increases in AA dosage, it decreased sharply. When the monomer proportion was small, it could not provide the needed monomers for the reaction in a timely manner, so the increasing amount of AA caused the active free radicals on the surface of CMC to react with the monomers and made the grafting reaction come to completion. When the AA dosage was sufficiently high, the generation of free monomers increased and the homopolymerization of the monomer AA played a major role. When the reaction was carried out to a certain level, a three-dimensional network of resin formed. The monomer free radical was surrounded by the early formation of a network and the liquidity and the collision rate of free radicals reduced, which was not conducive to the grafting reaction. Therefore, the optimal $m(\text{CMC}):m(\text{AA})$ ratio was 1:9.

Effect of potassium persulfate dosage

The effect of potassium persulfate dosage on the water absorbency was investigated at a $m(\text{CMC}):m(\text{AA})$ ratio of 1:9 and a degree of neutralization of 40%. The potassium persulfate dosages were 0.1, 0.3, 0.5, 0.7, and 0.9 g; with 2 g of carboxymethyl cellulose, the $m(\text{K}_2\text{S}_2\text{O}_8):m(\text{CMC})$ ratios were therefore 1:20, 3:20, 1:4, 7:20, and 9:20, respectively.

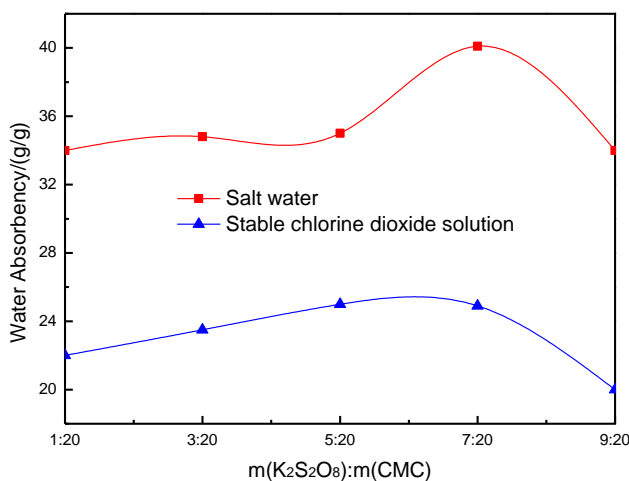


Fig. 5. Effect of $\text{K}_2\text{S}_2\text{O}_8$ dosage on water absorbency

The water absorbency increased with increasing $m(\text{K}_2\text{S}_2\text{O}_8):m(\text{CMC})$, up to 7:20. The water absorbency under these conditions was up to 40.1 g/g for salt water and 24.9 g/g for stable chlorine dioxide solution. This was because when the initiator dosage was small, the active free radicals generated on carboxymethyl cellulose in the reaction system decreased, the grafting reaction went on incompletely, and with the increase of initiator dosage, the number of radicals generated from CMC also increased; therefore, the water absorbency also was increased. However, when the initiator dosage reached a certain level, there were increasing opportunities for the monomer and initiator to react.

Potassium peroxydisulfate was not only the initiator of the cellulose graft copolymerization reaction, but also the initiator for the monomer acrylic acid, which also could increase the number of radicals and the rate of mono-polymerization. Otherwise, if the initiator dosage was too large, the reaction rate and the viscosity of the system would increase rapidly, causing the climbing phenomenon, also called the Weissenberg effect (Elson *et al.* 1982; Luo 1999). Therefore, the optimal $m(\text{K}_2\text{S}_2\text{O}_8):m(\text{CMC})$ ratio was 7:20.

Effect of neutralization degree

The effect of neutralization of AA on the water absorbency was investigated at a $m(\text{CMC}):m(\text{AA})$ ratio of 1:9 and a $m(\text{K}_2\text{S}_2\text{O}_8):m(\text{CMC})$ ratio of 7:20. The neutralization degree of AA was the percentage of carboxyl groups in the base-neutralized AA molecules. As shown in Fig. 6, the water absorbency of products increased with increasing neutralization degree, up to 40%. The water absorbency was up to 35.0 g/g for salt water and 24.9 g/g for stable ClO_2 solution (Fig. 6). However, when the degree of neutralization continued to increase, the absorbency decreased quickly until all the resin dissolved in water. The main reason for this was that when the degree of neutralization was lower, both the polymerization rate and exothermic rate were higher. An increase in the reaction temperature of the system would lead to a higher cross-linking degree and a

reduction of the free water held within the hydrogel. Moreover, the ionization degree of the -COOH group on the polymer chain was low due to the contracted state of the polymer network structure in the water, and the osmotic pressure and affinity were small, resulting in the small water absorbency (Gao *et al.* 2008).

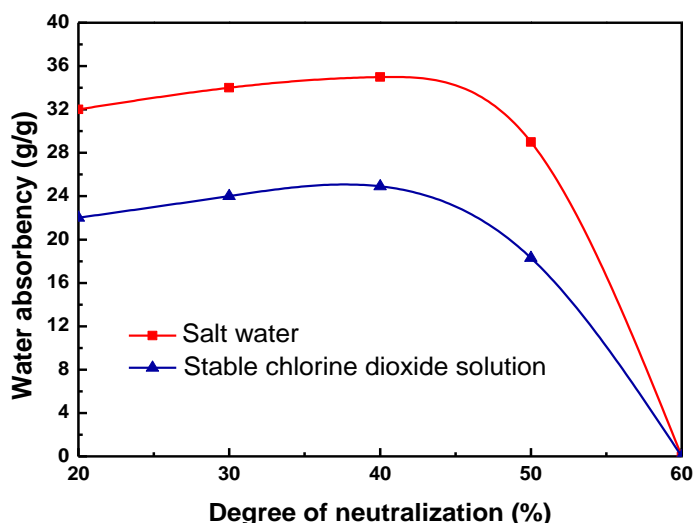


Fig. 6. Effect of neutralization on water absorbency

With increasing neutralization degree, the reaction rate slowed down; on the other hand, the number of hydrophilic groups (-COONa) increased. Because of the repelling interactions of the -COO- group, the molecular chain unbent and the network expanded, while the affinity was enhanced and the osmotic pressure increased, increasing the absorbency. However, when the neutralization degree reached a certain level, any additional degree of neutralization would reduce the activity of acrylic acid and slow the polymerization.

The reaction system should be neutral or weakly alkaline because it would completely produce sodium acrylate under the alkaline condition, causing the product to have poor water absorbency and retention and large water solubility; under certain conditions, no polymerization reaction occurred (Denes and Manolache 2004).

Finally, the optimal parameters were used to prepare the superabsorbent resin: plasma discharge power of 250 W, processing time of 90 s, pressure of 300 Pa, $m(\text{CMC}):m(\text{AA})$ ratio of 1:9, $m(\text{K}_2\text{S}_2\text{O}_8):m(\text{CMC})$ ratio of 1:4, and neutralization degree of 40%. Under these conditions, the resin achieved the largest absorbency of 38.5 g/g for salt water and 27.2 g/g for stable chlorine dioxide solution.

Structural Characterization of SAR

Infrared spectroscopic analysis

The carboxymethyl cellulose was analyzed by FTIR directly without pretreatment. The SAR was analyzed by FTIR after tableting with potassium bromide.

When comparing Fig. 7a and Fig. 7b, a new peak appeared near 1699.15 cm^{-1} , which was the stretching vibration absorption peak of the carbonyl group; it was neither attributed to AA nor CMC, but the result of mutual influence on each other, which showed that AA had been grafted to CMC.

The peaks at 1555.05 cm^{-1} and 1539.88 cm^{-1} were due to carbonyl asymmetric stretching vibration and symmetric stretching vibration for -COONa in sodium

polyacrylate salt. This showed that the product was formed from the graft polymerization of CMC and AA.

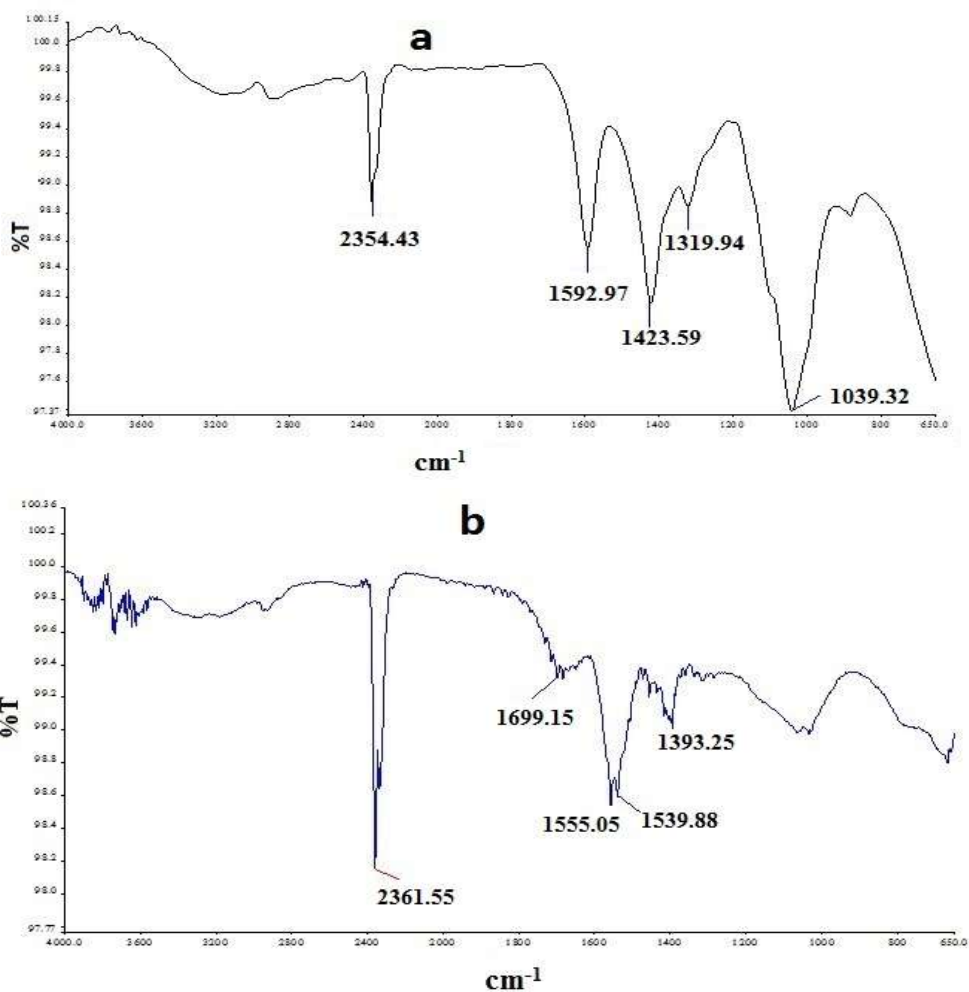


Fig. 7. FTIR images of (a) CMC prepared from bagasse pulp and (b) SAR prepared using the low-temperature plasma method

X-ray diffraction (XRD) analysis

Bleached bagasse pulp, CMC, and SAR were ground into powder and examined using XRD.

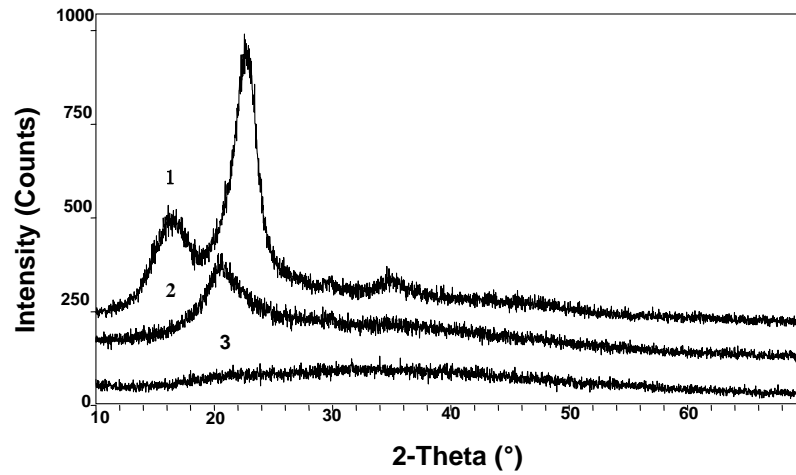
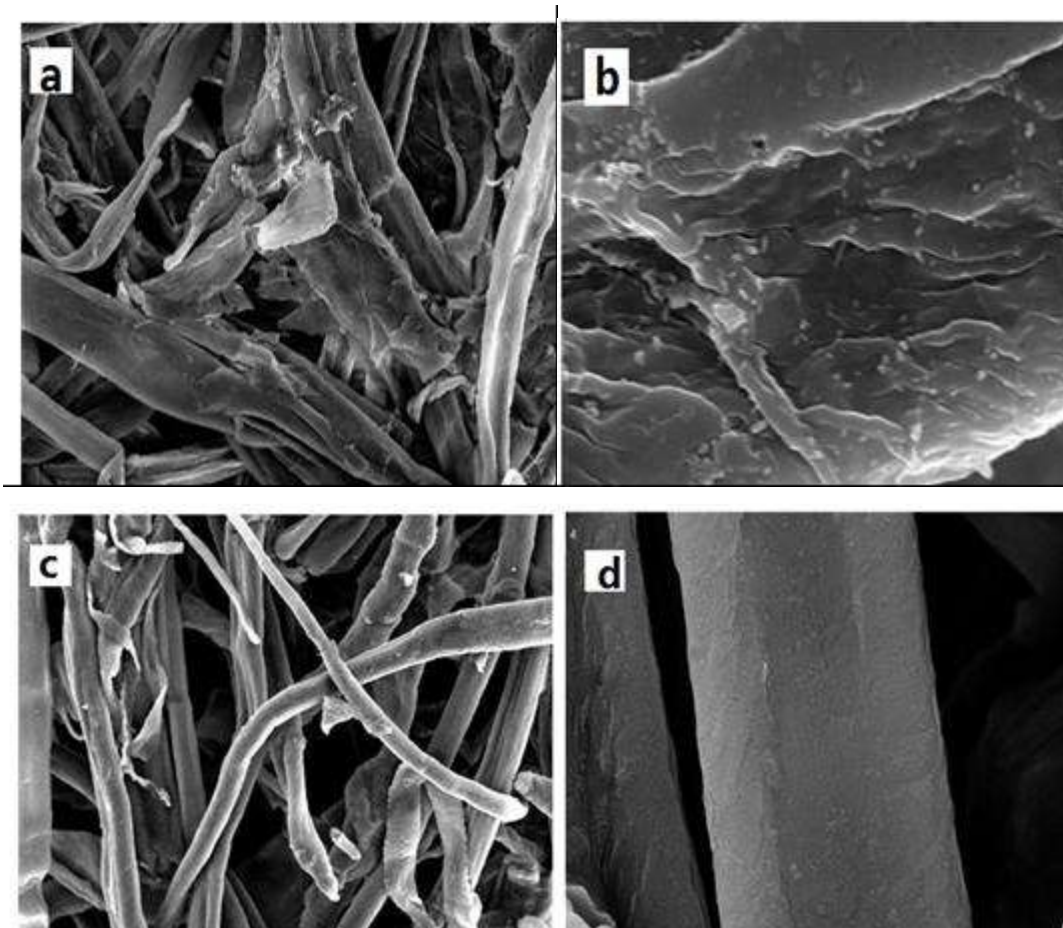


Fig. 8. XRD spectrum of BP, CMC, and SAR
Scanning electron microscopy (SEM)



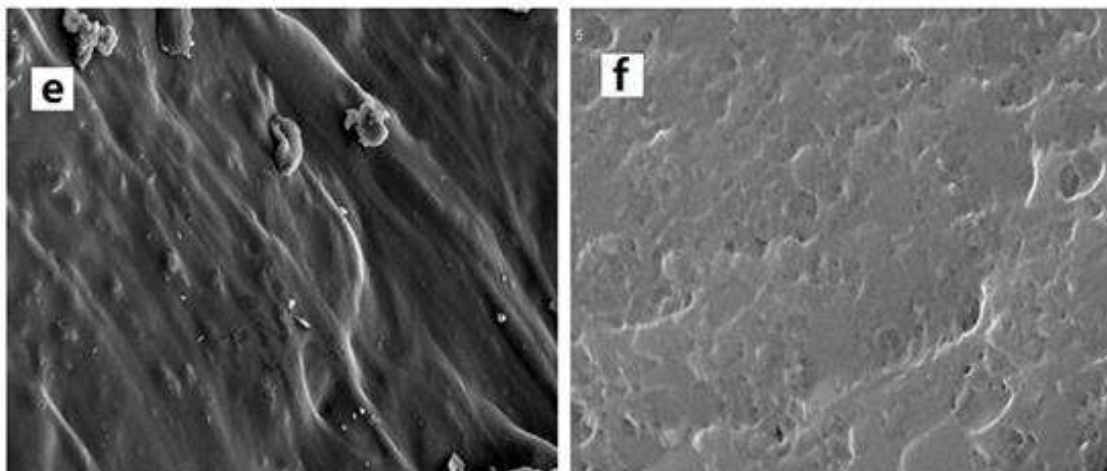


Fig. 9. SEM images of (a) bagasse pulp ($\times 500$), (b) bagasse pulp ($\times 5000$), (c) CMC ($\times 500$), (d) CMC ($\times 5000$), (e) dried superabsorbent resin ($\times 500$), and (f) dried superabsorbent resin ($\times 8000$)

When comparing the X-ray diffraction patterns of CMC and BP, broad peaks of CMC at 16° and 22° diffraction angles disappeared, but a broad peak appeared at the 20° diffraction angle; the smaller intensity of the peak showed that the etherification reaction reduced the crystallinity of the fiber. This occurred because the steric hindrance effect was changed after the carboxymethyl was introduced, causing the reduction of the regularity of carboxymethyl cellulose and the production of more amorphous regions, so the crystallinity was reduced. However, there still was a broad absorption peak; this showed that the crystal region of the CMC was not completely destroyed. When comparing the X-ray diffraction pattern of SAR with those of BP and CMC, it is clear that all the peaks disappeared; this showed that the resin did not have a regular crystalline structure, but was almost amorphous. The inherent crystal structure was destroyed primarily because AA was grafted to CMC.

Imaging

Figures 9a and 9b show that the original bagasse pulp fibers had various morphologies, and the surface was rough, with many impurities. Figures 9c and 9d show that CMC was significantly tapered, and the fiber surface was smooth and pure. The regular surface structure ensured the effect of using low-temperature plasma treatment on CMC, which initiated the active sites of the fiber surface in favor of the grafting reaction.

Figures 9c and 9d show that the surface of CMC was smooth and compact, and had no obvious holes, so its water absorption and retention was poor. Figure 9e and Fig. 9f show that there were some holes and cracks in the resin surface; also, a layered structure appeared, which benefitted the formation of the resin network structure, thereby improving the performance of the water absorbency and retention.

Thermal Behavior of SAR

Differential scanning calorimetry (DSC)

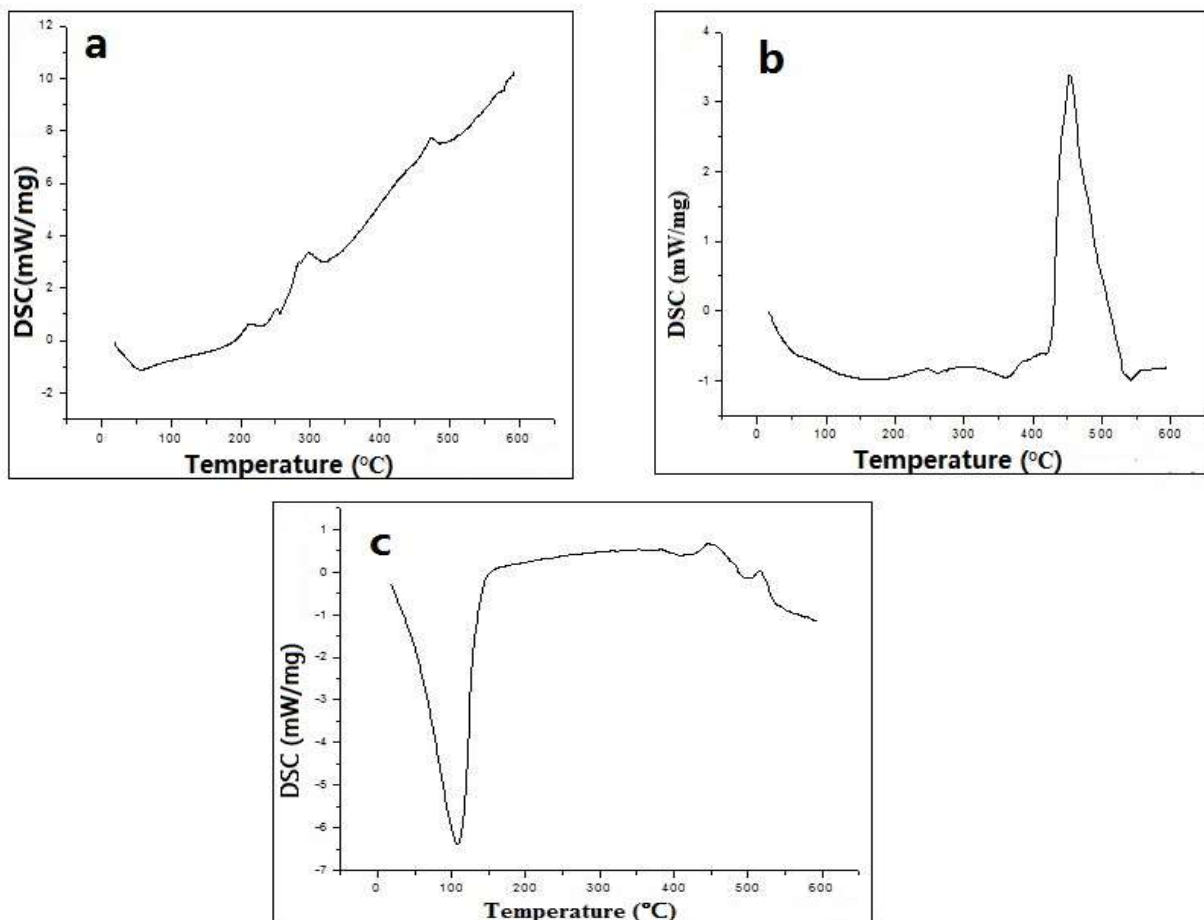


Fig.10. DSC images of (a) CMC, (b) dried SAR, and (c) wet SAR

Figure 10a shows a broad absorption peak in CMC at 60 °C, which can be attributed to the evaporation endothermic peak of water. Between 60 and 300 °C the curve continued to increase, which revealed that bagasse pulp was decomposing and releasing heat. Another absorption peak at 350 °C may be caused by heat absorption for the high-temperature decomposition reaction of CMC. At yet higher temperatures the CMC continued to decompose and release heat under high-temperature conditions, causing the DSC curve to rise continuously. Figure 10b shows that the dried SAR remained in the endothermic state, perhaps because of the fusion of acrylic acid in the branch; there was a large release peak between 435 and 540 °C, which was caused by the decomposition of SAR. Figure 10c shows that there was a very large endothermic peak between 50 and 150 °C for the wet SAR, which was the evaporation endothermic peak of water in the resin. No other peaks appeared before 400 °C, which indicated that the thermal stability of the resin was better than that of CMC alone.

CONCLUSIONS

1. Bleached bagasse pulp was used as the raw material. Superabsorbent resin (SAR) was synthesized from carboxymethyl cellulose by grafting with acrylic acid (AA) after low-temperature plasma treatment. The optimum preparation conditions were as follows: plasma discharge power of 250 W, processing time of 90 s, pressure of 300 Pa, $m(\text{CMC}):m(\text{AA})$ ratio = 1:9, $m(\text{K}_2\text{S}_2\text{O}_8):m(\text{CMC})$ ratio = 1:4, and neutralization degree of 40%. The largest water absorbency was as follows: 38.5 g/g for salt water and 27.2 g/g for stable chlorine dioxide solution.
2. The contrastive analysis of infrared spectroscopy for carboxymethylcellulose (CMC) and SAR showed that there were absorption peaks near 1699.15, 1555.05, and 1539.88 cm^{-1} due to carbonyl asymmetric stretching vibration and symmetric stretching vibration for $-\text{COONa}$ in sodium polyacrylate salt. This demonstrates that the product was synthesized by the graft polymerization of CMC and AA.
3. XRD analysis showed that there were two peaks at the 16° and 22° diffraction angles for bagasse pulp, and a smaller-intensity broad peak appeared at the 20° diffraction angle; this was because the etherification reaction reduced the degree of crystallinity of the samples. Comparing the X-ray diffraction diagrams of the SAR with bagasse pulp and CMC, it was clear that all the peaks disappeared, indicating that AA was grafted to CMC.
4. Comparison and analysis using scanning electron microscopy revealed that the surface of SAR not only contained some small dense holes and cracks, but also had a layered structure, which further explained the reason for the great improvement in water absorbency.
5. The scanning calorimetry test showed that the thermal stability of the resin was better than that of CMC alone.

ACKNOWLEDGMENTS

This work was supported by the Guangxi Natural Science Foundation (Grant nos. 2012GXNSFBA053026 and 2013jjFA20001).

REFERENCES CITED

- Denes, F. S., and Manolache, S. (2004). "Macromolecular plasma-chemistry: An emerging field of polymer science," *Progress in Polymer Science* 29(8), 815-885.
- Elson, T. P., Solomon, J., Nienow, A. W., and Pace, G. W. (1982). "The interaction of yield stress and viscoelasticity on the Weissenberg effect," *Journal of Non-Newtonian Fluid Mechanics* 11(1-2), 1-12.
- Gao, J. Z., Wang, A. X., Li Y., Fu, Y., Wu, J. L., Wang, Y. D., and Wang, Y. J. (2008). "Synthesis and characterization of superabsorbent composite by using glow discharge electrolysis plasma," *Reactive & Functional Polymers* 68(9), 1377-1383.
- Kabiri, K., Omidian, H., Hashemi, S. A., and Zohuriaan-Mehr, M. J. (2003). "Synthesis of fast-swelling superabsorbent hydrogels: Effect of crosslinker type and

- concentration on porosity and absorption rate,” *European Polymer Journal* 39(7), 1341-1348.
- Liu, J., Li, Q., Su, Y., Yue, Q. Y., Gao, B. Y., and Wang, R. (2013). “Synthesis of wheat straw cellulose-g-poly (potassium acrylate)/PVA semi-IPNs superabsorbent resin,” *Carbohydrate Polymers* 94(1), 539-546.
- Liu, J., Su, Y., Li, Q., Yue, Q. Y., and Gao, B. Y. (2013). “Preparation of wheat straw based superabsorbent resins and their applications as adsorbents for ammonium and phosphate removal,” *Bioresource Technology* 143, 32-39.
- Luo, X. L. (1999). “Numerical simulation of Weissenberg phenomena-The rod-climbing of viscoelastic fluids,” *Computer Methods in Applied Mechanics and Engineering* 180(3-4), 393-412.
- Ma, Z. H., Li, Q., Yue, Q. Y., Gao, B. Y., Xu, X., and Zhong, Q. Q. (2011). “Synthesis and characterization of a novel super-absorbent based on wheat straw,” *Bioresource Technology* 102(3), 2853-2858.
- Maithili, K., and Ram, M. (2003). “Disposable diapers: A hygienic alternative,” *Indian Journal of Pediatrics* 70(11), 879-881.
- Miao, Z. C., Wang, F. C., and Deng, D. (2012). “Preparation of cellulose-graft superabsorbent resin,” *Progress in Polymer Science* 557-559, 1018-1021.
- Park, K. H., Kim, H. I., and Das, R. P. (2005). “Selective acid leaching of nickel and cobalt from precipitated manganese hydroxide in the presence of chlorine dioxide,” *Hydrometallurgy* 78(3-4), 271-277.
- Sadeghi, M., and Hosseinzadeh, H. (2008). “Synthesis of starch-poly (sodium acrylate-coacrylamide) superabsorbent hydrogel with salt and pH-responsiveness properties as a drug delivery system,” *Journal of Bioactive and Compatible Polymers* 23(4), 381-404.
- Song, F. X., Wei, J. F., and He, T. S. (2009). “A method to repair concrete leakage through cracks by synthesizing super-absorbent resin in situ,” *Construction and Building Materials* 23(11), 386-391.

Article submitted: November 18, 2013; Peer review completed: February 8, 2014;
Revised version received and accepted: March 27, 2014; Published: April 8, 2014.